We are IntechOpen, the world's leading publisher of Open Access books Built by scientists, for scientists

6,900
Open access books available

185,000
International authors and editors

200M
Downloads

Our authors are among the

154
Countries delivered to

TOP 1%
most cited scientists

12.2%
Contributors from top 500 universities

WEB OF SCIENCE™

Selection of our books indexed in the Book Citation Index in Web of Science™ Core Collection (BKCI)

Interested in publishing with us?
Contact book.department@intechopen.com

Numbers displayed above are based on latest data collected.
For more information visit www.intechopen.com

14

Application of a Highly Reduced One-Dimensional Spring-Dashpot System to Inelastic SSI Systems Subjected to Earthquake Ground Motions

Masato Saitoh
Saitama University, Shimo-Okubo Sakura-Ku Saitama, Saitama
Japan

1. Introduction

Recent devastating earthquakes in many countries, particularly the 2010 Haiti earthquake (e.g., Eberhard et al., 2010) and the 2011 off the Pacific coast of Tohoku earthquake (e.g., Takewaki et al., 2011) in Japan, have caused severe damages to buildings and structures. The past and the recent seismic events have led us to attempt to improve technologies used in practical applications for evaluating the dynamic behavior of structural systems subjected to earthquake ground motions. To accomplish this, it is considered that an appropriate representation of soil-structure interaction (SSI) effects may be of great importance in earthquake engineering.

SSI has been studied since the late 19th century. Since then, developments in SSI science over the years have resulted in the latest SSI technologies (Kausel, 2010). In recent years, the effects of SSI have been taken into consideration in various practical numerical computations. For analyzing the dynamic response of SSI systems, a substructure method is often used for performing more efficient computations with lesser degrees of freedom (DOFs) rather than more comprehensive models with extremely large number of DOFs. In a substructure method, impedance functions (IFs) are generally used to represent the dynamic stiffness and damping of soil-foundation systems. Most IFs of soil-foundation systems exhibit various frequency-dependent characteristics; they usually occur as a result of the reflection and refraction of traveling waves originating from the foundations. Numerous studies associated with the frequency-dependent characteristics of IFs have been conducted over the past several years. IFs exhibit the following typical frequency-dependent characteristics: (a) slight oscillation shown in soil reaction and surface rigid foundations or embedded rigid foundations (Baranov, 1967; Beredugo & Novak, 1972; Novak, 1974; Novak et al., 1978; Veletsos & Dotson, 1988; Gazetas, 1991; Saitoh & Watanabe, 2004; Tileylioglu et al., 2011); (b) multiple oscillations typically exhibited in pile groups (Kaynia & Kausel, 1982; Dobry & Gazetas, 1988; Makris & Gazetas, 1993; Mylonakis & Gazetas, 1998); and (c) a cut-off frequency below which damping is negligible and above which damping increases rapidly (Novak & Nogami, 1977; Nogami & Novak, 1977; Kausel & Roesset, 1975; Elsabee &

Morray, 1977; Takemiya & Yamada, 1981). These studies have indicated that considering frequency dependency in the response analysis of structures can yield more accurate calculations in SSI systems.

In contrast to the findings of many of the latest studies of various foundations under diverse conditions and in recent numerical computations, frequency dependency in SSI systems has been recognized as a hindrance. In accordance with the recent performance-based seismic design of structures, nonlinearity in structural members, such as cracking, yielding, and collapse, needs to be considered in computations in order to predict the inelastic response of structural systems subjected to the expected earthquake waves. In calculating the response, step-by-step numerical procedures in the time domain are usually used with constitutive models, because the nonlinearity of structural members strongly depends upon the stress pass being integrated stepwise. Therefore, a conventional method for considering frequency dependency in the frequency domain cannot be applied. This has been one of the most important problems in structural engineering and geotechnical engineering over the past few decades.

Recently, various methods that are ready to use in practice have been proposed to overcome this issue, when frequency dependency in IFs and nonlinearity in structures are simultaneously taken into account. Basically, there are two main streams of thought in dealing with this problem. One is to use a method for transforming IFs into impulse responses in the time domain. The origins of this method date back to Wolf & Obernhuber, 1985, who developed a numerical method in the time domain in which the impulse response obtained from dynamic soil stiffness by using inverse Fourier transform was applied to the response analysis. Since this method was first developed in the 1980s, many transform methods in the time domain have been proposed and improved to overcome difficulties in various frequency dependencies in IFs (Wolf & Motosaka, 1989; Meek, 1990; Motosaka & Nagano, 1992; Hayashi & Katsukura, 1990). Nakamura (2006a; 2006b; 2008a; 2008b) has developed various sophisticated transform methods that can deal with strong frequency dependency in IFs, non-causal impedance with large hysteretic damping, and soil nonlinearity.

The other method for dealing with the SSI problem is the use of a lumped parameter model (LPM), which is considered to be a very powerful tool for solving this problem. In general, an LPM consists of springs, dashpots, and masses having frequency-independent coefficients. A particular combination of these elements can simulate a frequency-dependent impedance characteristic. The advantage of LPMs is that they can be easily incorporated into a conventional numerical analysis in the time domain, even under nonlinear conditions of superstructures. Time stepping methods that have conventionally been applied to structural analyses, such as the central difference method, Newmark's method, and Wilson's method—employed as conventional integration schemes—can be used with LPMs, while time-domain transform methods usually need a specific scheme to incorporate the impulse response into the response analysis.

From the viewpoint of construction schemes in LPMs, the existing LPMs can be categorized into three types: a) semi-empirical LPMs, b) systematic LPMs, and c) modal LPMs.

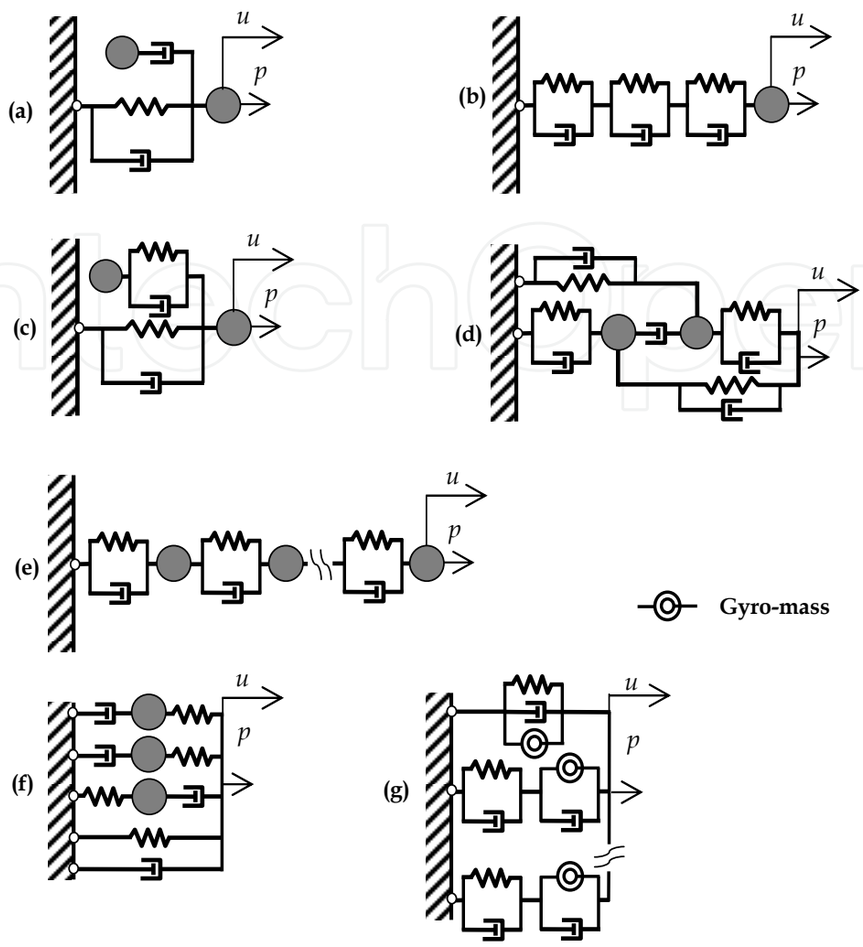

Fig. 1. Semi-empirical lumped parameter models proposed in previous studies [(a) Meek & Veletsos, 1974; Wolf & Somaini, 1986; (b) Nogami & Konagai, 1986; 1988; (c) de Barros & Luco, 1990; (d) Jean et al., 1990; (e) Wu & Chen, 2001; (f) Taherzadeh et al., 2009; and (g) Saitoh, 2011a].

In semi-empirical LPMs, mechanical elements such as springs, dashpots, and masses, which have frequency-independent coefficients, are arranged appropriately, depending on how significantly an optimal fit of the IFs obtained using LPMs with the corresponding target (exact) IFs can be achieved using specific arrangements. The values of the elements are usually determined by minimizing the errors from the target IFs. Meek & Veletsos, 1974, initially presented an LPM that represents the lateral and rocking impedance characteristics for a truncated semi-infinite cone that can be considered as an analog of an elastic half space. In an LPM, a mass has an additional DOF that is not directly attached to the foundation node but rather is connected to it through a dashpot, as shown in Fig. 1a. Wolf & Somaini, 1986, extended the above model to a rigid disk, an embedded cylinder, a rectangle, and a strip, and specified the coefficients of the elements comprising the foundations. Nogami & Konagai, 1986; 1988, represented the subgrade reaction of soil surrounding single piles by using three Voigt models connected in series (in the axial direction) and those with a mass (in the flexural direction), as shown in Fig. 1b. Alternative LPMs (de Barros & Luco, 1990

(Fig. 1c); Jean et al., 1990 (Fig.1d)) were proposed for a better fit to the impedance functions than the precedent LPMs. For a more concise usage of LPMs in practical applications, the coefficients of simple LPMs have been specified in tables for rigid foundations on the surface and with embedment in all translational and rotational motions (Wolf & Paronesso, 1992; Wolf, 1997). Wu & Chen, 2001, proposed an LPM consisting of a set of units in which each unit consists of a mass connected to a spring and a dashpot arranged in parallel, as shown in Fig. 1e. Wu & Chen, 2002, adopted the LPM to a simple SSI analysis for seismic excitations. Recently, other forms of LPMs have been proposed by researchers (Taherzadeh et al., 2009, (Fig. 1f); Khodabakhshi et al., 2011).

As described in Wolf, 1994; Wu & Chen, 2002; and Wu & Lee, 2002, however, the inclusion of any mass in an LPM becomes a drawback when an LPM is straightforwardly used in seismic excitations, that is, the driving forces at the foundation node induced by a foundation input motion differ from the corresponding forces by applying the same input motion at the bottom end (the far end) of an LPM because of the mass. This problem does not occur when an LPM consists of springs and dashpots. However, the lack of mass in an LPM tends to show difficulty in an appropriate fit to the exact impedance functions, and thus, a substantial increase in the number of elements and DOFs is necessary.

To overcome this issue, Saitoh, 2007, proposed an LPM that uses a gyro-mass element instead of an ordinary mass. The gyro-mass element generates a reaction force proportional to the relative acceleration of the nodes between which it is placed. The use of the gyro-mass element does not influence the driving forces acting at the foundation because the gyro-mass element does not generate any inertia force. An LPM with a gyro-mass element (GLPM) accomplishes a rapid change in frequency in IFs with a small number of elements without an ordinary mass. In Saitoh's study, two types of LPMs—*Type I* and *Type II* models—are presented for simulating IFs that have cut-off frequencies and frequency-dependent oscillations, respectively. In Saitoh, 2011a, the accuracy in the GLPMs was verified using an example of 2 × 4 pile groups embedded in a layered soil medium, supporting a 1DOF system having inelasticity in the structural member when subjected to ground motions. In his study, a more generalized GLPM, called "the *Type III* model" was proposed for a more appropriate fit (Fig. 1g).

In the development of semi-empirical LPMs, attempts have been made to obtain an easier and more systematic determination of the values for the coefficients in LPMs. A systematic procedure was first proposed by Wolf, 1991a; 1991b. In the procedure, the dynamic-stiffness coefficient is approximated as a ratio of two polynominals, which is then formulated as a partial-fraction expansion whose each term is represented by a discrete model comprising parallel-form LPMs, as shown in Fig. 2a. Wu & Lee, 2002, proposed series-form LPMs (Fig. 2b) formulated with a ratio of two polynominals approximating the flexibility functions (compliance functions) instead of using IFs. Moreover, Wu & Lee, 2004, alternatively proposed nested LPMs (Fig. 2c) based on a continued-fraction expansion instead of a partial-fraction expansion. The advantage of nested LPMs is that the configuration is independent of the soil-foundation systems being dealt with, whereas the previous series-form LPMs, which use the partial-fraction expansion, depend upon them. Another new systematic LPM (Fig. 2d) based on the continued-fraction expansion was proposed by Zhao & Du, 2008.

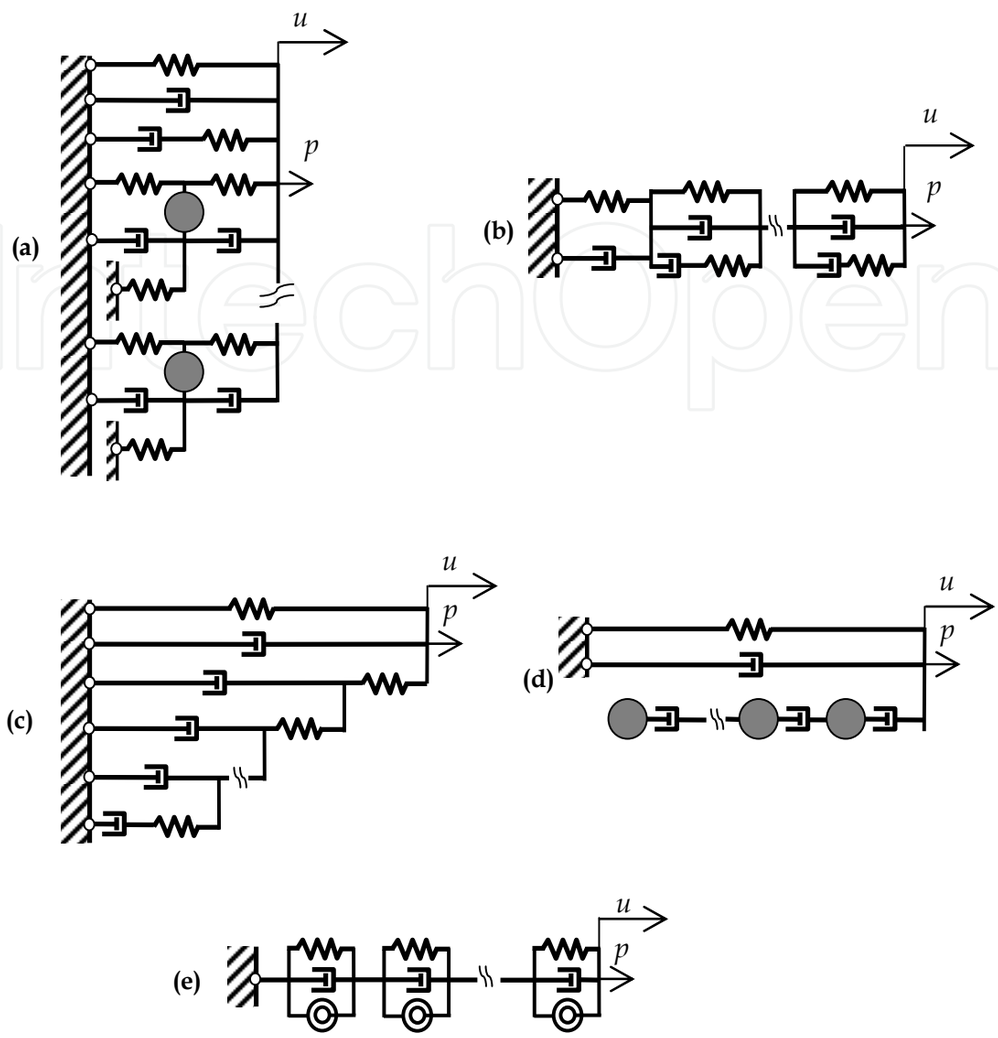

Fig. 2. Systematic lumped parameter models [(a) Wolf, 1991a; 1991b; (b) Wu & Lee, 2002; (c) Wu & Lee, 2004; and (d) Zhao & Du, 2008] and a modal LPM [(e) Saitoh, 2010a] proposed in previous studies.

The aforementioned LPMs need to approximate the target IFs by using specific functions such as the ratio of two polynominals in the case of systematic LPMs. Recently, two new transform methods for constructing an exact LPM from the original systems have been developed in the field of computational mechanics (Saitoh, 2010a; 2010b). In Saitoh, 2010a, an LPM consisting of units arranged in series—in which each unit consists of a spring, a dashpot, and a gyro-mass element arranged in parallel (Fig. 2e)—is formulated, i.e., calculated from a closed-form solution based on a modal expansion. In Saitoh's study, an LPM that represents the impedance characteristics at the extremity of a uniform, isotropic, and homogeneous rod supported by continuously distributed springs and dashpots (the Kelvin–Voigt model is assumed as a viscoelastic medium) was proposed. This method can be applied to systems where the conventional modal expansion is available for solving the differential equation of motion. In a later study (Saitoh, 2010b), a transformation procedure based on a conventional complex modal analysis was proposed in which the impedance

function in general linearly elastic systems with non-classical damping is transformed into an exact one-dimensional spring-dashpot system (1DSD) comprising units arranged in series. Each unit, which is directly related to each vibrating mode of the original system, is a parallel system consisting of a spring, a dashpot, and a unit having a spring and a dashpot arranged in series. The properties of the elements comprising the 1DSDs are automatically determined through the proposed procedure by using complex modal quantities. The advantage of 1DSDs is that 1DSD transformation offers compatibility with the merit of complex modal analysis, that is, a large number of units associated with high modes beyond the target frequency region can be removed from the 1DSDs as an approximate expression of impedance functions. Accordingly, a marked decrease in the computational domain size and time with the use of the 1DSDs can be achieved. Extremely complicated frequency dependency in impedance functions over a wide frequency range tends to appear in diverse technological applications, as exhibited in Saitoh, 2010b. In such cases, the approximation of the target IFs by using specific functions in the previous LPMs may encounter a certain limitation in terms of accuracy and may not be accomplished sufficiently. On the other hand, the 1DSDs transform procedure provides an exact LPM at the initial step, that is, we can adjust the number of DOFs (the number of units) in the reduced LPM by achieving a balance with the accuracy from the exact LPM. A transformation procedure for general linearly elastic systems with classical damping was also proposed in his recent study (Saitoh, 2011b).

Therefore, the main aim of this study is to verify the applicability of the transformation method of 1DSDs to SSI problems influenced by seismic excitations. This study deals with an application example of a four-story shear building supported by a shallow foundation embedded in layered soil resting on a rigid bedrock. The soil-foundation system is modeled using two-dimensional isoparametric finite elements, as shown in Fig. 4. In most previous studies, nonlinearity in structural members was not considered when verifying the performance of the proposed LPMs. In this study, therefore, the Clough model (Clough & Johnson, 1966), which has a bilinear skeleton curve, is applied to each inter-story in the building to compare the relationship between force and inter-storey drift obtained with 1DSDs with that obtained with the original finite element (FE) model.

2. Methodology for transforming structural systems with non-classical damping into reduced 1DSDs

This section presents an overview of the method for transforming structural systems into a 1DSD. The configuration of a 1DSD is shown in Fig. 3. In general, the impedance function $S_{IJ}(\omega)$ is defined as the ratio of the dynamic force P_J applied at an arbitrarily selected DOF (denoted as "*J*-th DOF") and the response displacement u_I at the same or another DOF (denoted as "*I*-th DOF"). Here ω is the excitation frequency. The properties of the elements comprising a 1DSD are derived from a proposed procedure based on complex modal analysis. In accordance with the detailed description in Saitoh, 2010b, the properties of the elements are evaluated using the stiffness matrix, the damping matrix, the mass matrix, and complex eigenvalues and eigenvectors. Once these values are obtained by a one-time complex modal calculation, the properties are automatically determined from the mathematical formula presented in Saitoh's study.

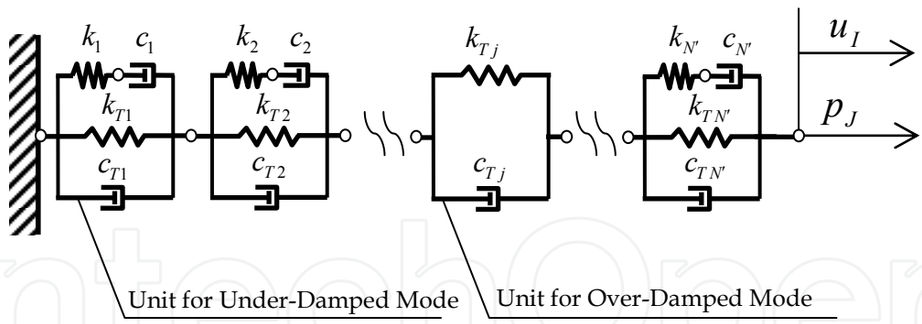

Fig. 3. One-dimensional lumped parameter model with spring and dashpot elements for simulating the impedance function $S_{IJ}(\omega) = p_J / u_I$ in general structural systems [Saitoh, 2010b].

In this method, the equations of motion of general linearly elastic structural systems comprising N DOFs are dealt with and are expressed by the following form:

$$[M]\{\ddot{u}\} + [C]\{\dot{u}\} + [K]\{u\} = \{p\} \tag{1}$$

where $[M]$, $[C]$, and $[K]$ are the mass matrix, damping matrix, and stiffness matrix, respectively, of the original structural systems. Each matrix has order $N \times N$. $\{u\}$ and $\{p\}$ are the response displacements and the external forces at the nodes, respectively, and each vector has order N. The dots denote partial derivatives with respect to time t. In this study, the damping matrix $[C]$ is assumed to be based on non-classical damping.

In complex modal analysis, the following $2N$ first-order equations are considered instead of the N second-order equations of Eq. 1:

$$[R]\{\dot{z}\} + [S]\{z\} = \{f\} \tag{2}$$

where

$$[R] = \begin{bmatrix} [C] & [M] \\ [M] & [0] \end{bmatrix}, \ [S] = \begin{bmatrix} [K] & [0] \\ [0] & -[M] \end{bmatrix}, \ \{z\} = \begin{Bmatrix} \{u\} \\ \{\dot{u}\} \end{Bmatrix}, \ \{f\} = \begin{Bmatrix} \{p\} \\ \{0\} \end{Bmatrix}.$$

The complex eigenvalues and eigenvectors can be obtained according to the conventional complex modal procedure. Each complex eigenvalue λ_n is known to have an eigenvalue $\bar{\lambda}_n$, which is the complex conjugate of λ_n; the corresponding vector $\{\varphi_n\}$ has a vector $\{\bar{\varphi}_n\}$, whose components are complex conjugates of those of $\{\varphi_n\}$. The eigenvectors are assembled compactly into a matrix using diagonal matrices $[\Omega]$ and $[\bar{\Omega}]$ comprising the eigenvalues λ_n and $\bar{\lambda}_n$, respectively, as

$$[\Psi] = \begin{bmatrix} [\varphi] & [\bar{\varphi}] \\ [\varphi][\Omega] & [\bar{\varphi}][\bar{\Omega}] \end{bmatrix} \tag{3a}$$

where

$$[\varphi]=\left[\{\varphi_1\} \quad \{\varphi_2\} \quad \cdots \quad \{\varphi_N\}\right] \tag{3b}$$

$$[\bar{\varphi}]=\left[\{\bar{\varphi}_1\} \quad \{\bar{\varphi}_2\} \quad \cdots \quad \{\bar{\varphi}_N\}\right] \tag{3c}$$

$$[\Omega]=\left[diag\,\lambda_n\right],\ n=1,2,\cdots,N \tag{3d}$$

$$\left[\bar{\Omega}\right]=\left[diag\,\bar{\lambda}_n\right],\ n=1,2,\cdots,N \tag{3e}$$

The matrix $[\Psi]$ is called the modal matrix. In general, $[\Psi]^T[R][\Psi]$ becomes a diagonal matrix owing to the orthogonality relationships. Here the upper N components of the matrix are denoted as α_n, while the lower N components are the complex conjugates of α_n, denoted as $\bar{\alpha}_n$.

At the end of the mathematical derivation in Saitoh's study, the properties of the elements can be determined using the following formula:

$$k_{Tn}=\frac{\sigma_n^2+\omega_{dn}^2}{2\left(G_n\sigma_n-R_n\omega_{dn}\right)} \tag{4}$$

$$c_{Tn}=\frac{1}{2G_n} \tag{5}$$

$$k_n=\frac{-\left(G_n^2+R_n^2\right)\omega_{dn}^2}{2G_n^2\left(G_n\sigma_n-R_n\omega_{dn}\right)} \tag{6}$$

$$c_n=\frac{-\left(G_n^2+R_n^2\right)\omega_{dn}^2}{2G_n\left(G_n\sigma_n-R_n\omega_{dn}\right)^2} \tag{7}$$

where $G_n+iR_n=\dfrac{\varphi_{nI}\varphi_{nJ}}{\alpha_n}$ and $G_n-iR_n=\dfrac{\bar{\varphi}_{nI}\bar{\varphi}_{nJ}}{\bar{\alpha}_n}$.

Here φ_{nI} and φ_{nJ} are the components of the n-th eigenvector at the I-th and J-th DOFs, respectively; $\bar{\varphi}_{nI}$ and $\bar{\varphi}_{nJ}$ are the complex conjugates of the components φ_{nI} and φ_{nJ}, respectively. σ_n is the n-th modal decay rate and ω_{dn} is the n-th damped natural circular frequency defined as

$$\lambda_n=-\sigma_n+i\omega_{dn} \tag{8}$$

$$\bar{\lambda}_n=-\sigma_n-i\omega_{dn} \tag{9}$$

In practice, over-damped modes often appear. In this case, eigenvalues λ_n are real and negative. In Saitoh, 2010b, it was mathematically derived that the impedance function associated with over-damped modes is expressed as a Kelvin–Voigt unit comprising spring k_{Tn} and dashpot c_{Tn}, as shown in Fig. 3.

$$k_{Tn} = \frac{\sigma_n}{G_n} \tag{10}$$

$$c_{Tn} = \frac{1}{G_n} \tag{11}$$

Note that over-damped modes generally appear with even numbers $2m$ in $2N$ modes, so the total unit number N changes to $N'(=N+m)$ when over-damped modes exist.

3. Application to soil-shallow foundation-structure system

3.1 FE model studied

This is the first application of a 1DSD to SSI problems. In principle, the dynamic response of the original structural systems, which have even inelasticity in their superstructures, can be correctly simulated using 1DSDs. However, the accuracy of the transfer functions and the time histories of the dynamic response of the structural system comprising 1DSDs have never been verified. In this section, therefore, a soil-shallow foundation system interacting with a multiple-DOF system with inelasticity is used for verification.

The overall system is shown in Fig. 4. A shallow foundation 10 m wide, 50 m long, and 2 m deep is embedded in layered soil up to the middle of the foundation. The elastic modulus of the foundation is assumed to be rigid, imposing unique displacements u_f and θ_f at the center of gravity in the horizontal and rotational directions, respectively. The mass and the mass moment of inertia of the foundation are $m_f = 1000$ t and $J_f = 8500$ tm², respectively. A four-story building supported by the foundation is represented by a 4-DOF system. The properties of the system are shown in the figure. In this study, the inelasticity in each story

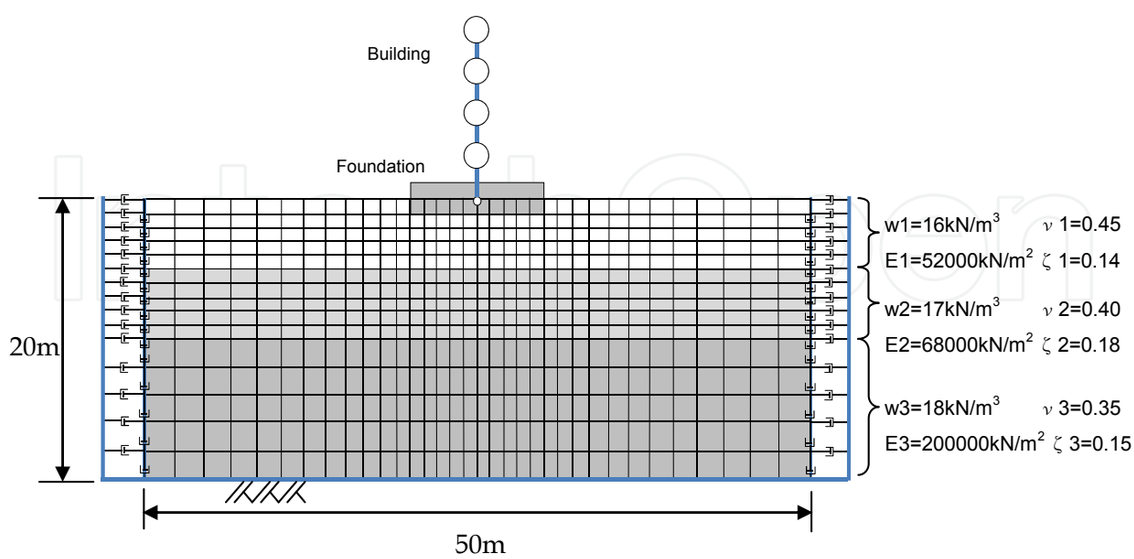

Fig. 4. Two-dimensional FE model for a soil-shallow foundation system supporting a four-story building. The unit weight, modulus of elasticity, Poisson's ratio, and damping ratio of the *i*-th soil layer are denoted as w_i, E_i, ν_i, and ζ_i, respectively.

is taken into account. The soil-foundation system is modeled using conventional two-dimensional rectangular isoparametric elements (Weaver et al., 1990), in which each element has eight DOFs. The soil strata are composed of three soil layers resting on a rigid bedrock. The bottom of the layered soil is fixed in the vertical and lateral directions, whereas a viscous boundary proposed by Lysmer and Kuhlemeyer, 1969, is applied to the sidewalls of the soil as a fictitious boundary that dissipates energy toward an infinite region of soil. The moduli of elasticity and the damping ratios of the soil shown in the figure are assumed to approximately account for the appreciable levels of strain during ground shaking. The total number of nodes comprising the isoparametric elements is 560, whereas the degrees of freedom minus the fixed degrees of freedom are 1,050. The thickness of the elements is the same as the length of the foundation (50 m) under a plane-strain condition.

3.2 Equations of motion of FE model with structures

In this model, the soil-foundation system consists of conventional isotropic elements, whereas the structural system comprising the superstructure and the mass of the foundation is discretized by springs, dashpots, and masses. Therefore, the global mass matrix, stiffness matrix, and damping matrix in the equations of motion of the total system are obtained by superimposing local matrices in both equilibrium equations. The details of the equations are described as follows.

The equations of motion of the soil-foundation system are expressed as

$$[M_G]\{\ddot{u}_G\}+[C_G]\{\dot{u}_G\}+[K_G]\{u_G\}=\{f_G\} \tag{12}$$

where $[M_G]$, $[C_G]$, and $[K_G]$ are the mass matrix, damping matrix, and stiffness matrix, respectively, of the soil-foundation system. $\{u_G\}$ and $\{f_G\}$ are the response displacements and the forces at the DOFs in the system, respectively. In this study, the damping matrix for each element is constructed on the basis of

$$[C_e]=\beta_l[K_e] \tag{13}$$

where

$$\beta_l=\frac{2\zeta_l}{\omega_1} \tag{14}$$

where $[C_e]$ and $[K_e]$ are the local damping matrix and stiffness matrix, respectively, of the isoparametric element; the parameter ζ_l is the damping ratio given in each soil layer at the fundamental natural frequency of the soil-foundation system; and ω_1 is the fundamental natural circular frequency of the undamped system. The damping ratio of each soil layer used in this model is shown in Fig. 4. In the FE model, the elastic modulus of the elements in the foundation is appreciably higher than that of the soil for realizing rigid body movement of the foundation. In addition, the mass density of the elements is negligible because the mass and the mass moment of inertia of the foundation are taken into account in the model of the building.

The equilibrium equation of the 4-DOF system connected with the rigid mass of the foundation is expressed as follows:

$$[M_I]\begin{Bmatrix}\{\ddot{u}_s\}\\ \ddot{u}_f\\ \ddot{\theta}_f\end{Bmatrix}+[C_I]\begin{Bmatrix}\{\dot{u}_s\}\\ \dot{u}_f\\ \dot{\theta}_f\end{Bmatrix}+[K_I]\begin{Bmatrix}\{u_s\}\\ u_f\\ \theta_f\end{Bmatrix}=\begin{Bmatrix}\{0\}\\ 0\\ 0\end{Bmatrix} \tag{15}$$

where

$$[M_I]=\begin{bmatrix} m_1 & 0 & 0 & 0 & 0 & m_1H_1\\ 0 & m_2 & 0 & 0 & 0 & m_2H_2\\ 0 & 0 & m_3 & 0 & 0 & m_3H_3\\ 0 & 0 & 0 & m_4 & 0 & m_4H_4\\ 0 & 0 & 0 & 0 & m_f & 0\\ m_1H_1 & m_2H_2 & m_3H_3 & m_4H_4 & 0 & J_f+\sum_{i=1}^{4}m_iH_i^2 \end{bmatrix} \tag{16}$$

$$[C_I]=\begin{bmatrix} \bar{c}_1 & -\bar{c}_1 & 0 & 0 & 0 & 0\\ -\bar{c}_1 & \bar{c}_1+\bar{c}_2 & -\bar{c}_2 & 0 & 0 & 0\\ 0 & -\bar{c}_2 & \bar{c}_2+\bar{c}_3 & -\bar{c}_3 & 0 & 0\\ 0 & 0 & -\bar{c}_3 & \bar{c}_3+\bar{c}_4 & -\bar{c}_4 & 0\\ 0 & 0 & 0 & -\bar{c}_4 & \bar{c}_4 & 0\\ 0 & 0 & 0 & 0 & 0 & 0 \end{bmatrix} \tag{17}$$

$$[K_I]=\begin{bmatrix} \bar{k}_1 & -\bar{k}_1 & 0 & 0 & 0 & 0\\ -\bar{k}_1 & \bar{k}_1+\bar{k}_2 & -\bar{k}_2 & 0 & 0 & 0\\ 0 & -\bar{k}_2 & \bar{k}_2+\bar{k}_3 & -\bar{k}_3 & 0 & 0\\ 0 & 0 & -\bar{k}_3 & \bar{k}_3+\bar{k}_4 & -\bar{k}_4 & 0\\ 0 & 0 & 0 & -\bar{k}_4 & \bar{k}_4 & 0\\ 0 & 0 & 0 & 0 & 0 & 0 \end{bmatrix} \tag{18}$$

where $\{u_s\}\left(=\{u_1 \quad u_2 \quad u_3 \quad u_4\}^T\right)$ are the absolute displacements of the DOFs in the superstructure, excluding the displacements related to the rotational response of the foundation, and $\bar{c}_i$ and $\bar{k}_i$ are the damping coefficient and the initial stiffness of each story in the superstructure, respectively. Here the suffix i is numbered from top to bottom. The damping matrix is constructed as Rayleigh damping by using the mass matrix (Eq. 16) and the stiffness matrix (Eq. 18) with a first and second modal damping constant of 0.05.

In fact, the DOF of the foundation in the rotational direction is incompatible with the DOFs in the FE model as no rotational DOF is explicitly considered at each node in the FE model. Therefore, the rotational displacement θ_f in the rigid mass of the foundation is transformed

in the FE model based on the geometrical relationship using the relative displacement at the center of the foundation to the displacement of the successive node located at the bottom of the foundation. In addition, the rotational moment is transmitted to the corresponding nodes in the FE model using an equivalent couple.

3.3 Transforming the original system into a 1DSD

According to the procedure shown in Section 3.1, the FE model is to be transformed into an equivalent 1DSD. Complex modal analysis is performed to obtain the fundamental quantities by which the properties of the elements in the 1DSD are determined. Complex modal analysis has commonly been used for estimating modal components. In this study, a conventional modal analysis (Foss, 1958) is used. First, the impedance function in the horizontal direction is considered. In this case, although movement of the foundation in the rotational direction may be restrained more accurately to obtain a net horizontal impedance function (by extracting the interactive components), it was not restrained in this study because the foundation is embedded in the soil only a little in the model. Thus, no difference was observed in either of the impedance functions.

The results of complex modal analysis show that the number of over-damped modes is 2,026, whereas that of under-damped modes is 74 (the total number of modes is 2,100). Therefore, the 1DSD consists of 2,026 Kelvin–Voigt units and 37 standard units. The results show that the lowest natural frequency is 2.11 Hz, whereas the highest frequency is 4,760,000 Hz. As described above, a significant advantage of a 1DSD is that the units comprising a 1DSD are associated with the vibration modes of the original structural system. Therefore, a small set of units associated with modes from the lowest order can appropriately express the dynamic characteristics of structural systems without using all units. Recently, Saitoh, 2011a, studied the influence of frequency dependency in pile-group impedance functions upon the elastic and inelastic responses of superstructures. The results indicate that the important frequency range is the dominant frequency of foundation input motions that excite the inertial structural systems. Figure 5 shows the time-history response acceleration at the ground surface calculated using the conventional one-dimensional wave propagation theory with the soil properties shown in Fig. 4. An observed earthquake record, 2004 Ojiya EW, is applied to the bottom soil layer. This response acceleration is used in the following calculations as the foundation input motion in this study, which indicates that, for simplicity, no adjustment for the kinematic interaction effects is conducted. The figure shows that the foundation input motion contains a wide range of frequency components showing the dominant frequency at around 1.4 Hz. The amplitude of acceleration ranges from 0 to 10 Hz. Therefore, this frequency range is considered to be the target frequency range in this study.

The modal analysis results show that 1,110 vibrating modes appear in this frequency range. In fact, many units associated with these modes contain a relatively large spring constant k_{Tn} than other units. These units can appreciably be removed provided the impedance functions of the reduced 1DSD are in sufficient agreement with those of the original system. In this study, only 35 units (12 under-damped modes and 23 over-damped modes) remain after applying a threshold to the spring constant k_{Tn} of 1.0×10^{10} kN/m, above which the corresponding unit is removed. This threshold is adjusted on the basis of both the number of

units remaining suitable for effective computation and the accuracy in the approximation of impedance functions. The properties of the reduced 1DSD are shown in Table 1. Figure 6 shows a comparison of the impedance functions K_{hh} obtained from the reduced 1DSD with those obtained with the FE model. The results indicate that the impedance functions obtained from the 1DSD agree closely with those obtained with the FE model within the target frequency range.

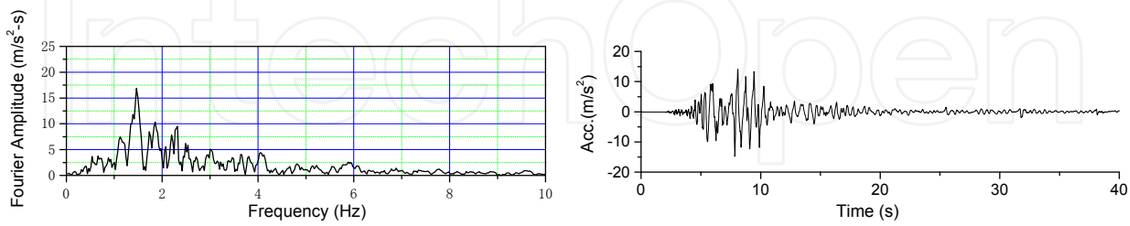

Fig. 5. Fourier amplitude and time history of the foundation input motion.

The impedance functions K_{rr} in the rotational direction are obtained along similar lines to the impedance functions in the horizontal direction. To obtain the relationship between rotational moment and displacement in the FE model, the center of the foundation is fixed in the horizontal and vertical directions and lateral force is applied to the successive node at the bottom of the foundation. The results of the complex modal analysis show that the number of over-damped modes is 2,018, while that of under-damped modes is 78 (total number of modes is 2,096). Therefore, the 1DSD consists of 2,018 Kelvin–Voigt units and 39 standard units. In this direction, 44 units (27 under-damped modes and 17 over-damped modes) comprise the reduced 1DSD after applying a threshold to the spring constant k_{Tn} in the rotational direction of 7.0×10^{10} kNm/rad. The properties of the reduced 1DSD are shown in Table 2. The resultant impedance functions in the rotational direction at the center of the foundation are shown in Fig. 6. Although a slight difference in the impedance functions appear in a high-frequency region when compared with those with the FE model, fairly close agreement can be observed over the target frequency range, on the whole.

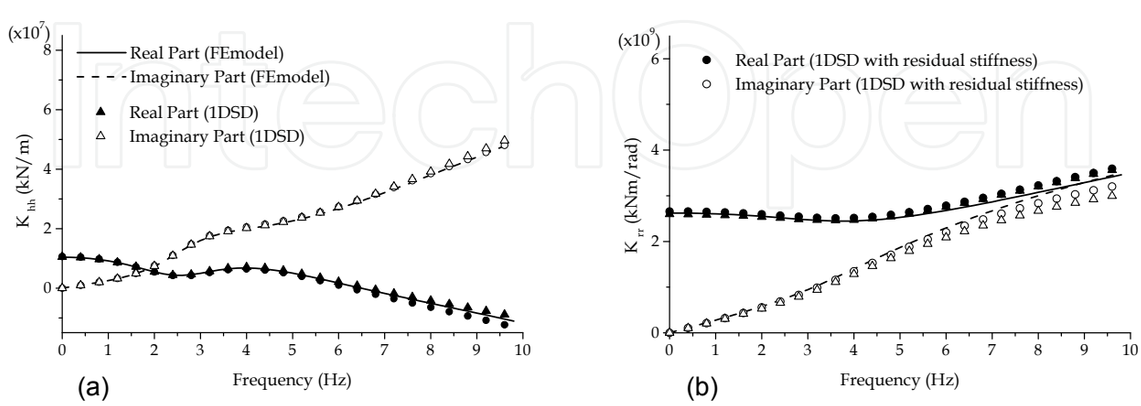

Fig. 6. Impedance functions of a soil-shallow foundation system using 1DSDs and 1DSDs with residual stiffness [(a) K_{hh} in the horizontal direction and (b) K_{rr} in the rotational direction]. Results obtained from the original FE model are shown for comparison.

In Saitoh, 2010b, a mechanical element associated with residual stiffness R_{IJ} was proposed to improve the accuracy of the reduced 1DSD. Residual stiffness has often been applied to approximate expressions of structural systems in conventional modal analysis. The residual stiffness representing the stiffness of high-frequency modes is expressed as

$$\frac{1}{R_{IJ}} = \sum_{n=l+1}^{N'} \frac{1}{\overline{K}_{nIJ}} = \frac{1}{\overline{K}_{l+1IJ}} + \frac{1}{\overline{K}_{l+2IJ}} + \cdots + \frac{1}{\overline{K}_{N'IJ}} \tag{19}$$

where

$$\text{For under-damped modes:} \quad \overline{K}_{nIJ} = \frac{\sigma_n^2 + \omega_{dn}^2}{2\left(\sigma_n G_n - \omega_{dn} R_n\right)} \tag{20}$$

$$\text{For over-damped modes:} \quad \overline{K}_{nIJ} = \frac{\sigma_n}{G_n} \tag{21}$$

where l is the maximum mode number considered in the 1DSDs without residual stiffness.

The residual stiffness R_{IJ} can be incorporated into the 1DSDs as a mechanical element arranged in series with the 1DSDs. The residual stiffnesses in both horizontal and rotational

Mode (n)	1	2	3	4	5	6
k_n	-4.5692E+08	3.7591E+08	1.0618E+09	-5.1042E+08	-1.6506E+10	0.0000E+00
c_n	-6.6604E+06	2.1711E+07	7.9324E+07	-3.9891E+07	2.6594E+07	0.0000E+00
k_{Tn}	1.9143E+07	-4.2683E+08	-1.4162E+09	6.8531E+08	4.7634E+07	8.2805E+09
c_{Tn}	7.4465E+06	-1.1586E+07	-2.0610E+07	7.6590E+06	-2.5143E+07	2.0113E+08
	7	8	9	10	11	12
k_n	0.0000E+00	0.0000E+00	0.0000E+00	0.0000E+00	0.0000E+00	0.0000E+00
c_n	0.0000E+00	0.0000E+00	0.0000E+00	0.0000E+00	0.0000E+00	0.0000E+00
k_{Tn}	1.9166E+09	2.9441E+09	6.5445E+09	8.8819E+09	1.9163E+09	6.5327E+09
c_{Tn}	4.6386E+07	7.1043E+07	1.5783E+08	2.1356E+08	4.5797E+07	1.5576E+08
	13	14	15	16	17	18
k_n	0.0000E+00	0.0000E+00	0.0000E+00	0.0000E+00	0.0000E+00	0.0000E+00
c_n	0.0000E+00	0.0000E+00	0.0000E+00	0.0000E+00	0.0000E+00	0.0000E+00
k_{Tn}	1.1882E+09	5.3841E+09	4.9079E+09	1.7577E+09	8.5567E+09	4.9203E+09
c_{Tn}	2.8224E+07	1.2766E+08	1.1612E+08	4.1497E+07	2.0073E+08	1.1436E+08
	19	20	21	22	23	24
k_n	0.0000E+00	0.0000E+00	0.0000E+00	0.0000E+00	0.0000E+00	0.0000E+00
c_n	0.0000E+00	0.0000E+00	0.0000E+00	0.0000E+00	0.0000E+00	0.0000E+00
k_{Tn}	7.8980E+09	7.1101E+08	6.3409E+09	3.0631E+09	2.2748E+09	1.7152E+09
c_{Tn}	1.7967E+08	1.6147E+07	1.4262E+08	6.8550E+07	5.0782E+07	3.7956E+07
	25	26	27	28	29	30
k_n	0.0000E+00	0.0000E+00	0.0000E+00	-1.8100E+10	0.0000E+00	-3.0252E+08
c_n	0.0000E+00	0.0000E+00	0.0000E+00	3.9047E+08	0.0000E+00	-3.5556E+06
k_{Tn}	5.6713E+09	2.0277E+08	5.6121E+09	5.6507E+09	4.3924E+09	2.4506E+08
c_{Tn}	1.2154E+08	4.2003E+06	1.1373E+08	-1.0463E+08	8.4557E+07	7.5807E+06
	31	32	33	34	35	Resi. Stif.
k_n	-9.4744E+09	-3.4928E+09	-4.8323E+09	-6.2970E+09	-1.1486E+10	0.0000E+00
c_n	5.7840E+07	4.4528E+07	-2.1066E+07	3.2994E+07	-7.5059E+07	0.0000E+00
k_{Tn}	6.6702E+08	6.8297E+08	6.2645E+08	4.3951E+08	7.6216E+09	-6.6866E+08
c_{Tn}	-3.5218E+07	-1.7234E+07	3.5920E+07	-1.8667E+07	2.2991E+08	0.0000E+00

*units: kN/m for k_n and k_{Tn}; and kNsec/m for c_n and c_{Tn}

Table 1. Properties of mechanical elements in reduced 1DSDs in the horizontal direction

directions are presented in Table 1 and Table 2, respectively. In Fig. 6, the impedance functions of the residual 1DSDs with the residual stiffness are plotted. An appreciable improvement can be seen in the high-frequency region when incorporating the residual stiffness in both directions.

3.4 Dynamic response of structural system in frequency domain

In this section, the dynamic response of the structural system computed by using the reduced 1DSDs in the frequency domain is verified by comparing it with the dynamic response obtained with the original FE model. The complete structural system using the 1DSDs in both horizontal and rotational directions is shown in Fig. 7. The properties of the superstructure are summarized in Table 3. The reduced 1DSDs obtained above are connected with each DOF in the foundation, as shown in the figure. The equations of motion of the structural system can be easily constructed using Eq. 15 with conventional spring-dashpot matrices (details are described in Saitoh, 2010b) expressing the reduced 1DSDs. The resultant equilibrium equations of the total system can be formulated as

Mode (n)	1	2	3	4	5	6
k_n	-8.7367E+10	-3.2511E+10	5.9885E+11	-8.9724E+10	-2.0509E+12	-8.2557E+10
c_n	-8.6002E+08	-3.2912E+08	-5.3876E+09	7.6112E+08	-2.2854E+09	8.3561E+08
k_{Tn}	6.3069E+09	3.8708E+09	-3.4692E+10	5.3955E+09	4.5267E+09	8.6083E+09
c_{Tn}	9.9889E+08	4.1663E+08	3.9650E+09	-5.4771E+08	2.4152E+09	-4.9286E+08
	7	8	9	10	11	12
k_n	0.0000E+00	-6.2547E+09	0.0000E+00	0.0000E+00	0.0000E+00	0.0000E+00
c_n	0.0000E+00	-2.1604E+08	0.0000E+00	0.0000E+00	0.0000E+00	0.0000E+00
k_{Tn}	2.9016E+10	1.0142E+10	3.3727E+10	4.2553E+10	1.7739E+10	4.1057E+10
c_{Tn}	6.8559E+08	1.5672E+08	7.7893E+08	9.5936E+08	3.7922E+08	8.7675E+08
	13	14	15	16	17	18
k_n	0.0000E+00	-5.5850E+10	0.0000E+00	0.0000E+00	-1.1840E+12	3.6129E+09
c_n	0.0000E+00	9.3275E+08	0.0000E+00	0.0000E+00	3.3843E+09	1.5195E+08
k_{Tn}	1.9758E+10	1.3439E+10	5.1907E+10	1.5146E+10	2.1723E+10	-6.6498E+09
c_{Tn}	4.0089E+08	-3.1988E+08	1.0150E+09	2.9275E+08	-2.7039E+09	-5.0781E+07
	19	20	21	22	23	24
k_n	-1.0096E+09	-8.9520E+09	-3.2909E+09	-1.1530E+12	3.8877E+10	-7.9236E+08
c_n	-2.2987E+07	-1.0163E+08	-3.8159E+07	-3.6097E+09	6.5584E+09	-7.6230E+06
k_{Tn}	2.4822E+09	1.2331E+10	4.6047E+09	6.8295E+10	-4.5729E+10	2.1613E+09
c_{Tn}	3.2532E+07	3.0091E+08	1.0301E+08	5.3063E+09	-5.3463E+07	3.8351E+07
	25	26	27	28	29	30
k_n	0.0000E+00	0.0000E+00	0.0000E+00	-3.5501E+09	0.0000E+00	-1.8681E+09
c_n	0.0000E+00	0.0000E+00	0.0000E+00	-6.3417E+06	0.0000E+00	-2.5699E+06
k_{Tn}	-4.6466E+10	-3.5291E+10	-4.6258E+10	2.0957E+09	-4.9346E+10	2.2527E+09
c_{Tn}	-4.6411E+08	-2.1706E+08	-1.9382E+08	1.5135E+07	-1.6920E+08	9.2640E+06
	31	32	33	34	35	36
k_n	0.0000E+00	0.0000E+00	-1.4155E+09	-1.7451E+09	8.1243E+06	-2.3990E+06
c_n	0.0000E+00	0.0000E+00	-3.9743E+06	-2.7057E+06	1.5958E+04	-4.7181E+03
k_{Tn}	-2.9367E+10	-1.0747E+10	1.3208E+10	9.9997E+09	-1.9771E+10	5.1191E+09
c_{Tn}	-6.6288E+07	-2.3854E+07	2.3000E+07	2.5153E+07	-3.9248E+07	9.6705E+06
	37	38	39	40	41	42
k_n	0.0000E+00	-3.4634E+08	-2.6621E+09	-7.3699E+06	-1.6447E+07	-3.2997E+08
c_n	0.0000E+00	-5.8881E+05	-3.8641E+06	-1.3444E+04	-2.8127E+04	-5.2243E+05
k_{Tn}	1.2511E+10	4.5378E+10	3.0996E+10	6.1565E+10	3.8787E+09	3.1127E+10
c_{Tn}	2.3189E+07	8.9426E+07	7.0953E+07	1.1015E+08	7.0887E+06	5.8484E+07
	43	44	Resi. Stif.			
k_n	0.0000E+00	0.0000E+00	0.0000E+00			
c_n	0.0000E+00	0.0000E+00	0.0000E+00			
k_{Tn}	-5.8039E+10	-3.1792E+10	-1.0587E+10			
c_{Tn}	-9.5838E+07	-5.0192E+07	0.0000E+00			

*units: kNm/rad for k_n and k_{Tn}; and kNm sec/rad for c_n and c_{Tn}

Table 2. Properties of mechanical elements in reduced 1DSDs in the rotational direction

$$[M_T]\{\ddot{u}\}+[C_T]\{\dot{u}\}+[K_T]\{u\}=\{0\} \tag{22}$$

where

$$\{u\}=\left[u_s\ u_f\ \ u_1\ u_2\cdots u_i\cdots u_m\ \theta_f\ \theta_1\ \theta_2\cdots\theta_i\cdots\theta_n\right]^T \tag{23}$$

where the mass matrix $[M_T]$, the damping matrix $[C_T]$, and the stiffness matrix $[K_T]$ are the resultant matrices formed by superimposing the partial matrices. u_i and θ_i are the displacements at the DOFs in the reduced 1DSDs. The maximum DOFs in both directions are represented by m $(=47)$ and n $(=71)$, respectively. In order to estimate the response of the structural system, the absolute displacements are expressed by the sum of the displacements of the inertial response and the input motion, as follows:

$$\{u\}=\{U\}+\{U_g\} \tag{24}$$

where

$$\{U\}=\left[U_s\ U_f\ \ U_1\ U_2\cdots U_i\cdots 0\ \Theta_f\ \Theta_1\ \Theta_2\cdots\Theta_i\cdots 0\right]^T \tag{25}$$

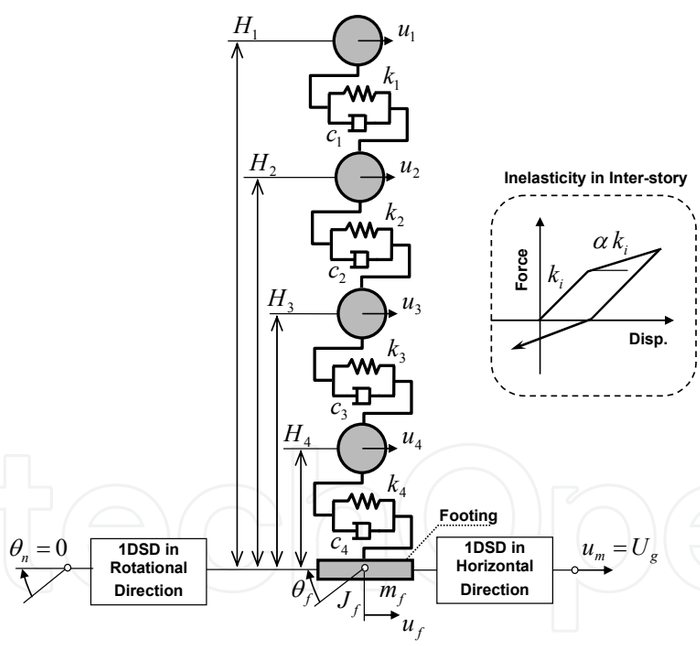

Fig. 7. Numerical model representing complete structural system.

Story No.	Units	1	2	3	4
Mass m_i	t	750	750	750	750
Stiffness k_i	kN/m	2000000	2000000	2000000	2000000
Height H_i	m	12	9	6	3
Yield Strength p_i	kN	15000	30000	33000	44000

Table 3. Properties of four-story building

$$\{U_g\} = \left[U_g\ U_g\ U_g\ U_g \cdots U_g \cdots U_g\ \Theta_g\ \Theta_g\ \Theta_g \cdots \Theta_g \cdots \Theta_g\right]^T \tag{26}$$

where U_g and Θ_g are the foundation input motions to the inertial system in the horizontal and rotational directions, respectively. In this study, the foundation input motion in the rotational direction Θ_g is neglected as the amplitude is negligible because of the shallow embedment of the foundation in the soil. Substituting Eq. 24 into Eq. 22 leads to

$$[M_T]\{\ddot{U}\} + [C_T]\{\dot{U}\} + [K_T]\{U\} = -[M_T]\{\ddot{U}_g\} \tag{27}$$

The comparison is performed using the transfer functions (TFs) of the dynamic responses of the superstructure with respect to the foundation input motion defined as $T_{sa} = \left(\ddot{U}_1 + \ddot{U}_g + H_1\ddot{\Theta}_f\right)/\ddot{U}_g$ for absolute acceleration. The TFs of the footing are also computed. They are defined as $T_{ha} = \left(\ddot{U}_f + \ddot{U}_g\right)/\ddot{U}_g$ and $T_{ra} = H_1\ddot{\Theta}_f/\ddot{U}_g$ for the absolute acceleration associated with the horizontal and rotational motions, respectively.

Figure 8 shows the real part and the imaginary part of the transfer functions of the structural systems defined above. The figure indicates that the transfer functions obtained with the reduced 1DSDs are compatible with those obtained with the original FE model. This implies that 1DSDs with almost one-tenth of the DOFs in the original system can correctly represent the impedance functions in the target frequency region. Here the transfer functions obtained using the 1DSDs with residual stiffness are not presented as negligibly small differences that appeared in the impedance functions.

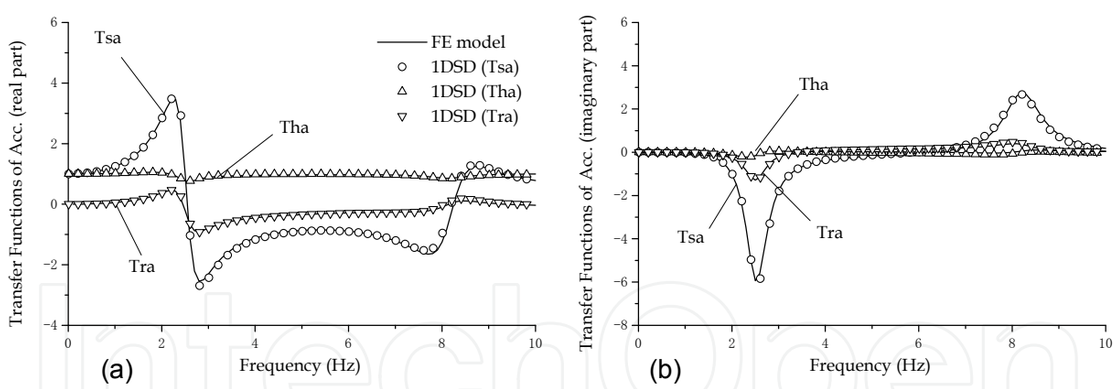

Fig. 8. Comparisons of the transfer functions of the structural system computed using 1DSDs without residual stiffness and the original FE model [(a) real part and (b) imaginary part].

3.5 Dynamic response of structural system in time domain

3.5.1 Elastic response of structural system

In the previous section, it was shown that a structural system with reduced 1DSDs can correctly simulate the transfer functions in the real part and the imaginary part in the frequency domain. This implies that the time-history response of a structural system having linearly elastic members can be appropriately calculated using 1DSDs. In this section, the

time-history response of a structural system with 1DSDs when subjected to foundation input motion is computed and compared with that obtained with the original FE model. An attempt is then made to compute the time-history response of the structural system with inelasticity in the superstructure.

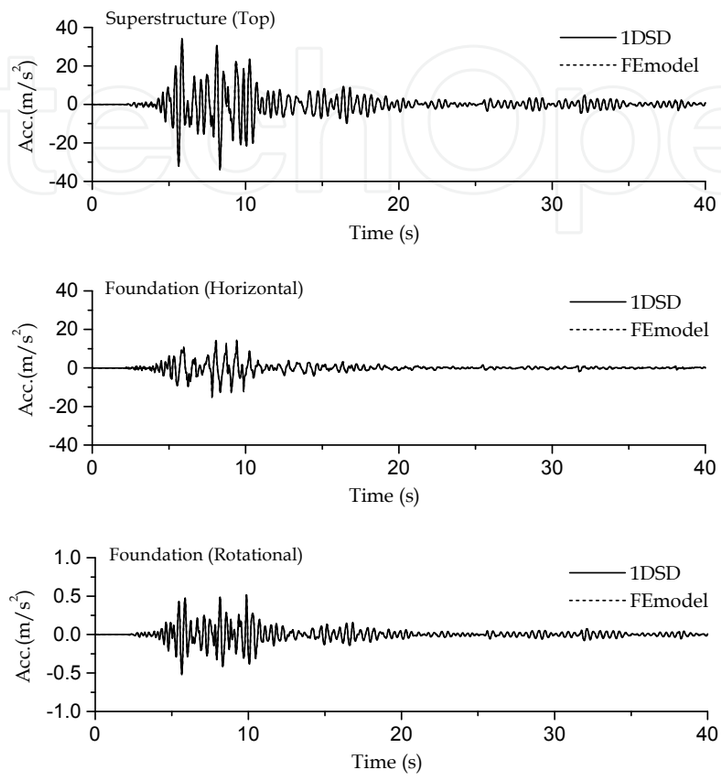

Fig. 9. Time-history response accelerations of superstructure and footing in the horizontal and rotational directions when subjected to ground motion associated with 2004 Ojiya EW by using 1DSDs and the original FE model.

The time-history analysis is performed on the basis of Eq. 27 by using Newmark's β method ($\beta = 1/4$) as a numerical integration scheme in which the time interval Δt is 0.001 s. The acceleration response at the ground surface shown in Fig. 5 is applied as the foundation input motion. Here the response accelerations defined in the previous section (the same definitions as in the transfer functions) are calculated. Figure 9 shows the time-history responses of the acceleration of the structural systems using reduced 1DSDs without residual stiffness. The figure shows that the time histories of the 1DSDs are compatible with those of the original FE model.

Note that a structural system using 1DSDs with residual stiffness cannot be obtained correctly because the dynamic response of the system is not converged (the response increases oscillatory with time). This implies that the structural system becomes unstable, which is attributed to the residual stiffness components. The unit for residual stiffness in the horizontal and rotational directions comprises only a negative stiffness, as shown in Table 1 and Table 2. This negative stiffness could be a drawback to stabilizing the dynamic response

of structures, although the units can achieve better agreement with the impedance functions of the original systems in the frequency domain.

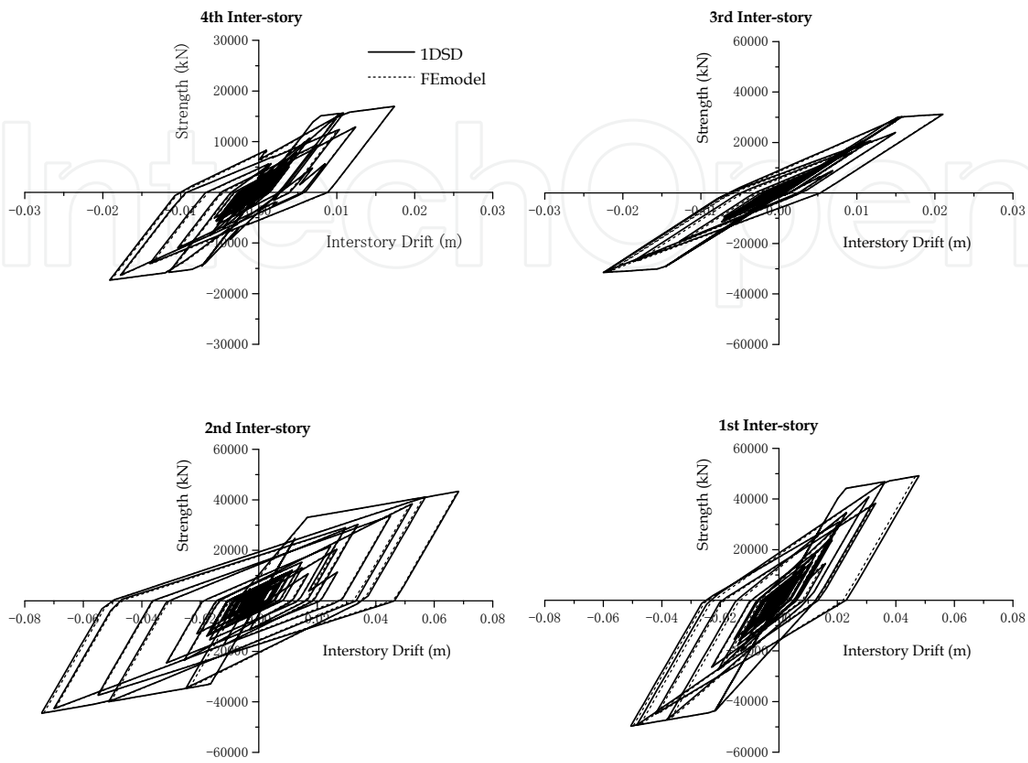

Fig. 10. Relationship between shear force and inter-story drift in each story when subjected to ground motion associated with 2004 Ojiya EW by using 1DSDs and the original FE model.

3.5.2 Inelastic response of structural system

Comparisons are extended to the structural system to allow inelasticity in the superstructure. The inelasticity of the superstructure is represented by the Clough model (Clough & Johnson, 1966), which is generally used to model reinforced concrete members. The spring of the superstructure has a bilinear skeleton curve in which the ratio of tangent stiffness to initial stiffness is assumed to be 0.1, as shown in Fig. 7. The yield strength p_i in each story is presented in Table 3. In this study, the modified Newton–Raphson method is applied to calculate the nonlinear response of the system.

Figure 10 shows the relationship between shear force and inter-story drift in each story. Figure 11 shows the time-history responses of the displacement of the foundation u_f and $H_1\theta_f$ in the horizontal and rotational directions, respectively. The results indicate that although a slight difference appears in the relationship between shear force and inter-story drift in the first inter-storey, the inelastic responses obtained with the 1DSDs show sufficiently close agreement with those obtained from the original FE model. From a practical viewpoint, a dominant advantage is that the computational time can be

considerably reduced by transforming the original system into 1DSDs. According to a rough measurement using the author's PC (CPU 3.40 GHz, RAM 3.00 GB), the inelastic responses shown above were obtained in about 11,965 s with the original FE model, while those with 1DSDs were obtained in about 68 s.

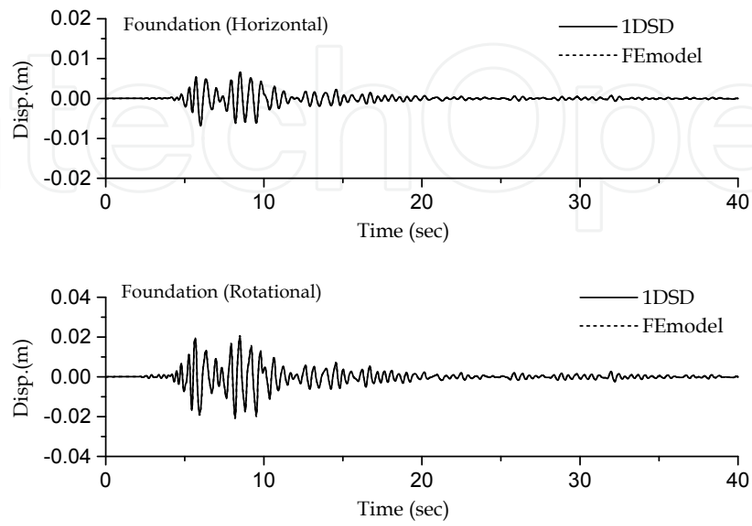

Fig. 11. Time-history response displacements of the foundation in the horizontal and rotational directions when subjected to ground motion associated with 2004 Ojiya EW by using 1DSDs and the original FE model.

4. Conclusion

This study demonstrates the transformation procedure using a 1DSD for a multi-story building supported on a shallow foundation embedded in layered soil. In accordance with the conventional modal concept, the reduced 1DSDs in both horizontal and rotational directions are constructed with a small number of units associated with important modes in the target frequency region in this application example. The impedance functions obtained with the 1DSDs correctly simulate the impedance functions of the original FE model. The transfer functions of the structural systems in the frequency domain using the 1DSD show fairly good agreement with those obtained with the FE model. The time-history responses of structures in both linearly elastic and inelastic cases can be simulated using the 1DSDs. The results indicate that a significant decrease in the structural system with the 1DSD lead to a marked decrease in the computational time taken for the results. Therefore, it may be concluded that 1DSD transformation is effective and efficient for numerical computations in SSI problems influenced by ground motions.

5. References

Baranov, V. A. (1967). On the calculation of excited vibrations of an embedded foundation (*in Russian*), *Voprosy Dynamiki I Prochnocti*, Polytechnical Institute of Riga, No. 14, pp. 195-209

Beredugo, Y. O. & Novak, M. (1972). Coupled horizontal and rocking vibration of embedded footings, *Can. Geotech. J.*, 9 (4), pp. 477-497

de Barros, F. C. P. & Luco, J. E. (1990). Discrete models for vertical vibrations of surface and embedded foundations, *Earthquake Engineering and Structural Dynamics*, 19, pp. 289–303

Clough, R. W. & Johnson, S. B. (1966). Effect of stiffness degradation on earthquake ductility requirements, *The second Earthquake Engrg. Sym., Proc.*, pp. 227-232

Dobry, R. & Gazetas, G. (1988). Simple method for dynamic stiffness and damping of floating pile groups, *Geotechnique*, 38 (4), pp. 557-674

Elsabee, F. & Morray, J. P. (1977). Dynamic behavior of embedded foundation, *Research Report,* R77-33, Dep. of Civil Engrg., MIT. Cambridge, Mass.

Foss, K. A. (1958). Co-ordinates which uncouple the equations of motion of damped linear dynamic systems, *Journal of Applied Mechanics*, 57, pp. 361–364

Gazetas, G. (1991). Formulas and charts for impedances of surface and embedded foundations, *J. Geotech. Engrg.* ASCE, 117(9), pp. 1363-1381

Hayashi, Y. & Katsukura, Y. (1990). Effective time domain soil–structure interaction analysis based on FFT algorithm with causality condition, *Earthquake Engineering and Structural Dynamics*, 19, pp. 693-708

Jean, W. Y., Lin, T. W. & Penzien, J. (1990). System parameters of soil foundations for time domain dynamic analysis. *Earthquake Engineering and Structural Dynamics*, 19, pp. 541-553

Kausel, E. (2010). Early history of soil-structure interaction, *Soil Dynamics and Earthquake Engineering*, 30, pp. 822-832

Kausel, E. & Roesset, J. M. (1975). Dynamic Stiffness of Circular Foundations, *J. Engrg. Mech. Div.*, ASCE, Vol. 101, No. EM6, pp. 770-1731

Kaynia, A. & Kausel, E. (1982). Dynamic stiffness and seismic response of pile groups, *Research Report*, R82-03, Dept. of Civil Engrg., MIT, Cambridge, Mass.

Khodabakhshi, P., Jahankhah, H., & Ghannad, M. A. (2011). A discrete model for response estimation of soil-structure systems with embedded foundations, *Earthquake Engineering and Engineering Vibration*, 10 (2), pp. 263-276

Lysmer, J. & Kuhlemeyer, R. L. (1969). Finite dynamic model for infinite media, *J. Eng. Mech. Div.*, ASCE, 95, pp. 859-877

Makris, N. & Gazetas, G. (1993). Displacement phase differences in a harmonically oscillating pile, *Geotechnique*, 43 (1), pp. 135-150

Meek, J. W. & Veletsos, A. S. (1974). Simple models for foundations in lateral and rocking motion, *Proc.*, 5*th World Conf. on Earthquake Engrg.*, 2, Rome, Italy, pp. 2610-2613

Meek, J. W. (1990). Recursive analysis of dynamic phenomena in civil engineering, *Bautechnik*, 67, pp. 205–210, (in German)

Motosaka, M. & Nagano, M. (1992). Recursive evaluation of convolution integral in nonlinear soil–structure interaction analysis and its applications, *Journal of Structural and Construction Engineering (AIJ)*, 436, pp. 71-80, (in Japanese)

Mylonakis, G. & Gazetas, G. (1998). Vertical vibration and additional distress of grouped piles in layered soil, *Soils and Foundations*, JGS, 38 (1), pp. 1-14

Nakamura, N. (2006a). A Practical method to transform frequency dependent impedance to time domain, *Earthquake Engineering and Structural Dynamics*, 35(2), pp. 217-234

Nakamura, N. (2006b). Improved methods to transform frequency dependent complex stiffness to time domain, *Earthquake Engineering and Structural Dynamics*, 35(8), pp. 1037-1050

Nakamura, N. (2008a). Transform Methods for Frequency Dependent Complex Stiffness to Time Domain Using Real or Imaginary Data Only, *Earthquake Engineering and Structural Dynamics*, 37(4), pp. 495-515

Nakamura, N. (2008b). Time history Response Analysis Considering Dynamic Stiffness with Both Frequency and Strain Dependencies, *J. of Eng. Mechanics*, ASCE, 134(4), pp. 530-541

Nogami, T. & Novak, M. (1977). Resistance of soil to a horizontally vibrating pile, *Earthquake Engineering and Structural Dynamics*, 5, pp. 249-261

Nogami, T. & Konagai, K. (1986). Time domain axial response of dynamically loaded single piles, *J. Engrg. Mech.*, ASCE, 112(11), pp. 1241-1252

Nogami, T. & Konagai, K. (1988). Time domain flexural response of dynamically loaded single piles, *J. Engrg. Mech.*, ASCE, 114(9), pp. 1512-1525

Novak, M. (1974). Dynamic stiffness and damping of piles, *Can. Geotech. J.*, 11, pp. 574-598.

Novak, M. & Nogami, T. (1977). Soil-pile interaction in horizontal vibration, *Earthquake Engineering and Structural Dynamics*, 5, pp. 263-281

Novak, M., Nogami, T., Konagai, K., & Aboul-Ella, F. (1978). Dynamic soil reactions for plane strain case, *J. Engrg. Mech.*, ASCE, 104(4), pp. 953-959

Saitoh, M. & Watanabe, H. (2004). Effects of flexibility on rocking impedance of deeply embedded foundation, *Journal of Geotechnical and Geoenvironmental Engineering*, ASCE, 130(4), pp. 438-445

Saitoh, M. (2007). Simple model of frequency-dependent impedance functions in soil-structure interaction using frequency-independent elements, *Journal of Engineering Mechanics*, ASCE, 133(10), pp. 1101-1114

Saitoh, M. (2010a). Lumped parameter models representing impedance functions at the interface of a rod on a viscoelastic medium, *Journal of Sound and Vibration*, 330, pp. 2062-2072

Saitoh, M. (2010b). Equivalent One-Dimensional Spring-Dashpot System Representing Impedance Functions of Structural Systems with Non-Classical Damping, *CMES: Computer Modeling in Engineering & Sciences*, 67(3), pp. 211-238

Saitoh, M. (2011a). On the performance of lumped parameter models with gyro-mass elements for the impedance function of a pile-group supporting a single-degree-of-freedom system, *Earthquake Engineering and Structural Dynamics*, DOI: 10.1002/eqe.1147

Saitoh, M. (2011b). A one-dimensional lumped parameter model representing impedance functions in general structural systems with proportional damping, International Journal for Numerical Methods in Engineering, DOI: 10.1002/nme.3323

Taherzadef, R., Clouteau, D., & Cottereau, R. (2009). Simple formulas for the dynamic stiffness of pile groups, *Earthquake Engineering and Structural Dynamics*, 38(15), pp. 1665-1685

Takemiya, H. & Yamada, Y. (1981). Layered soil-pile-structure interaction, *Earthquake Engineering and Structural Dynamics*, 9, pp. 437-452

Takewaki, I., Murakami, S., Fujita, K., Yoshitomi, S., Tsuji, M. (2011). The 2011 off the Pacific coast of Tohoku earthquake and response of high-rise buildings under long-period ground motions, *Soil Dynamics and Earthquake Engineering*, doi:10.1016/j. soildyn. 2011. 06. 001

Tileylioglu, S., Stewart, J. P., & Nigbor, R. L. (2011). Dynamic stiffness of a shallow foundation from forced vibration of a field test structure, *Journal of Geotechnical and Geoenvironmental Engineering*, Vol. 137 (4), pp. 344-353

Eberhard, M. O., Baldridge, S., Marshall, J., Mooney, W., G. J., Rix (2010). T*he Mw 7.0 Haiti Earthquake of January 12, 2010*, USGS/EERI Advance Reconnaissance Team: Team Report V.1.1

Veletsos, A. S. & Dotson, K. W. (1988). Horizontal impedances for radially inhomogeneous viscoelastic soil layers, *Earthquake Engineering and Structural Dynamics*, 16, pp. 947-966

Weaver, J. W., Timoshenko, S. P., & Young, D. H. (1990). Vibration Problems in Engineering, Fifth Edition, Wiley Interscience

Wolf, J. P. (1994). Foundation Vibration Analysis Using Simple Physical Models. Englewood Cliffs, NJ, Prentice-Hall

Wolf, J. P. & Obernhuber, P. (1985). Nonlinear soil-structure-interaction analysis using dynamic stiffness or flexibility of soil in the time domain, *Earthquake Engineering and Structural Dynamics*, 13, pp. 195-212

Wolf, J. P. & Motosaka, M. (1989). Recursive evaluation of interaction force of unbounded soil in the time domain, *Earthquake Engineering and Structural Dynamics*, 18, pp. 345-363

Wolf, J. P. & Somaini, D. R. (1986). Approximate dynamic model of embedded foundation in time domain, *Earthquake Engineering and Structural Dynamics,* 14, pp. 683-703

Wolf, J. P. & Paronesso, A. (1992). Lumped-parameter model for a rigid cylindrical foundation embedded in a soil layer on rigid rock, *Earthquake Engineering and Structural Dynamics*, 21, pp. 1021-1038

Wolf, J. P. (1997). Spring-dashpot-mass models for foundation vibrations. *Earthquake Engineering and Structural Dynamics*, 26, pp. 931-949

Wolf, J. P. (1991a). Consistent lumped-parameter models for unbounded soil: physical representation, *Earthquake Engineering and Structural Dynamics*, 20(1), pp. 11-32

Wolf, J. P. (1991b). Consistent lumped-parameter models for unbounded soil: frequency-independent stiffness, damping and mass matrices, *Earthquake Engineering and Structural Dynamics*, 20(1), pp. 33-41

Wu, W. H. & Chen, C. Y. (2001). Simple lumped-parameter models of foundation using mass-spring-dashpot oscillators, *J Chin Inst Eng*, 24(6), pp. 681-97

Wu, H. W. & Chen, C. Y. (2002). Simplified Soil-structure Interaction Analysis Using Efficient Lumped-parameter Models for Soils, *Soils and Foundations*, 42, pp. 41-52

Wu, W. H. & Lee, W. H. (2002). Systematic lumped-parameter models for foundations based on polynomial-fraction approximation. *Earthquake Engineering and Structural Dynamics*, 31, pp. 1383-1412

Wu, H. W. & Lee, H. W. (2004). Nested Lumped-parameter Models for Foundation Vibrations, *Earthquake Engineering and Structural Dynamics*, 33, pp. 1051-1058

Zhao, M. & Du, X. (2008). High-order lumped-parameter model for foundation based on continued fraction, Beijing, 14WCEE

IntechOpen

IntechOpen

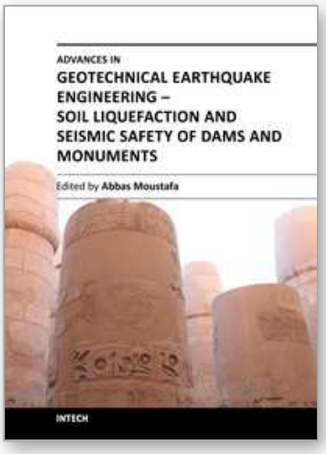

Advances in Geotechnical Earthquake Engineering - Soil Liquefaction and Seismic Safety of Dams and Monuments

Edited by Prof. Abbas Moustafa

ISBN 978-953-51-0025-6
Hard cover, 424 pages
Publisher InTech
Published online 10, February, 2012
Published in print edition February, 2012

This book sheds lights on recent advances in Geotechnical Earthquake Engineering with special emphasis on soil liquefaction, soil-structure interaction, seismic safety of dams and underground monuments, mitigation strategies against landslide and fire whirlwind resulting from earthquakes and vibration of a layered rotating plant and Bryan's effect. The book contains sixteen chapters covering several interesting research topics written by researchers and experts from several countries. The research reported in this book is useful to graduate students and researchers working in the fields of structural and earthquake engineering. The book will also be of considerable help to civil engineers working on construction and repair of engineering structures, such as buildings, roads, dams and monuments.

How to reference

In order to correctly reference this scholarly work, feel free to copy and paste the following:

Masato Saitoh (2012). Application of a Highly Reduced One- Dimensional Spring-Dashpot System to Inelastic SSI Systems Subjected to Earthquake Ground Motions, Advances in Geotechnical Earthquake Engineering - Soil Liquefaction and Seismic Safety of Dams and Monuments, Prof. Abbas Moustafa (Ed.), ISBN: 978-953-51-0025-6, InTech, Available from: http://www.intechopen.com/books/advances-in-geotechnical-earthquake-engineering-soil-liquefaction-and-seismic-safety-of-dams-and-monuments/application-of-a-highly-reduced-one-dimensional-spring-dashpot-system-to-inelastic-ssi-systems-subje

INTECH
open science | open minds

InTech Europe
University Campus STeP Ri
Slavka Krautzeka 83/A
51000 Rijeka, Croatia
Phone: +385 (51) 770 447
Fax: +385 (51) 686 166
www.intechopen.com

InTech China
Unit 405, Office Block, Hotel Equatorial Shanghai
No.65, Yan An Road (West), Shanghai, 200040, China
中国上海市延安西路65号上海国际贵都大饭店办公楼405单元
Phone: +86-21-62489820
Fax: +86-21-62489821

© 2012 The Author(s). Licensee IntechOpen. This is an open access article distributed under the terms of the Creative Commons Attribution 3.0 License, which permits unrestricted use, distribution, and reproduction in any medium, provided the original work is properly cited.